

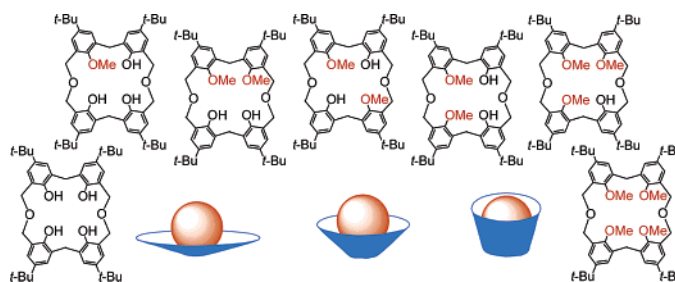
Methyl Ether Derivatives of *p*-*tert*-Butyl[3.1.3.1]homooxalixarene. Formation, Structure, and Complexes with Quaternary Ammonium Ions

Bernardo Masci,^{*,†} Stefano Levi Mortera,[†] Daniela Persiani,[†] and Pierre Thuéry[‡]

Dipartimento di Chimica and IMC-CNR, Università "La Sapienza", Box 34—Roma 62, P.le Aldo Moro 5, 00185 Roma, Italy, and SCM (CNRS URA 331), CEA/Saclay, Bât. 125, 91191 Gif-sur-Yvette, France

bernardo.masci@uniroma1.it

Received September 14, 2005



The whole set (five compounds) of partially *O*-methylated products of *p*-*tert*-butyl[3.1.3.1]homooxalixarene, currently named *p*-*tert*-butyltetrahomodioxalix[4]arene, have been prepared. Their structure has been investigated in solution through NMR techniques and in the solid state by single-crystal X-ray diffraction. A systematic investigation, extended to the parent tetraphenol and to the tetramethyl ether derivative, has been carried out on the complexation of tetramethylammonium, acetylcholine, *N*-methylpyridinium, and tetraethylammonium picrate in CDCl₃. The observed trends in the binding and in the selectivity of the strictly related hosts could be analyzed on the basis of the varying importance of intramolecular hydrogen bonding and its effects on the conformation of the free and of the complexed ligands. On increasing the number of methyl ether functions, the cone conformation appears to be relatively less stable but deeper, so small organic cations can be more effectively encircled.

Introduction

The name [3.1.3.1]homooxalixarene indicates the oxygenated homologues of calixarenes¹ in which two distal methylene groups bridging the aromatic units in the typical calix[4]arene series are replaced by CH₂OCH₂ groups.² The above macrocyclic system is currently indicated as a tetrahomodioxalix[4]arene,³ but the introduction of the isomer with proximal

substitution,⁴ which can be safely designated as a [3.3.1.1]-homooxalixarene, suggests to abandon the ambiguous name.⁵ We reported on some tetra-*O*-alkylated *p*-*tert*-butyl[3.1.3.1]-homooxalixarenes^{4,6} and No and co-workers have recently reported on tetra-*O*-alkylated *p*-phenyl analogues,⁷ while only one report can be found on a partially *O*-alkylated compound.⁸ In a systematic investigation on the tetramethyl ether derivatives of all the possible *p*-*tert*-butylhomooxalix[4]arenes, the [3.1.3.1]homooxalixarene proved to be the best suited host for the inclusion of tetramethylammonium ion;⁴ moreover,

* To whom correspondence should be addressed; Fax: +39 06 490631.

† Università "La Sapienza".

‡ CEA/Saclay.

(1) (a) Gutsche, C. D. *Calixarenes*; The Royal Society of Chemistry: Cambridge, England, 1989. (b) Gutsche, C. D. *Calixarenes Revisited*; The Royal Society of Chemistry: Cambridge, England, 1997. (c) *Calixarenes: A Versatile Class of Macrocyclic Compounds*; Vicens, J., Böhmer, V., Eds.; Kluwer: Dordrecht, The Netherlands, 1991. (d) *Calixarenes 2001*; Asfari, Z., Böhmer, V., Harrowfield, J., Vicens, J., Eds.; Kluwer: Dordrecht, The Netherlands, 2001.

(2) Masci, B. In ref 1d.

(3) (a) Dhawan, B.; Gutsche, C. D. *J. Org. Chem.* **1983**, *48*, 1536. (b) Masci, B. *Tetrahedron* **2001**, *57*, 2841.

(4) Masci, B.; Finelli, M.; Varrone, M. *Chem.—Eur. J.* **1998**, *4*, 2018.

(5) Typical homooxalixarenes feature only CH₂OCH₂ and CH₂ bridges; therefore, in the abridged names we use, the numbers in brackets are 3 or 1 and there is no need to explicitly indicate the number of aromatic rings, the number of oxygen atoms, or the location of the oxygen atom in the bridges. Moreover, we use the well-established term "homooxalixarene" rather than the term "oxalixarene", which could suggest the presence of O bridges by analogy with the important class of thialixarenes; see: Hosseini, M. W. In ref 1d.

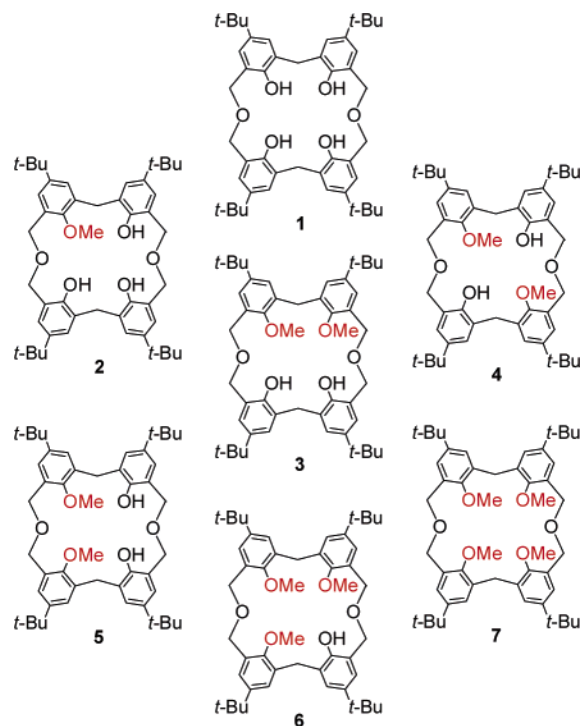
(6) De Iasi, G.; Masci, B. *Tetrahedron Lett.* **1993**, *34*, 6635.

TABLE 1. Product Distribution in the Methylation of Compound 1

run	reactants (concn, mmol L ⁻¹)	solvent ^a	time, h	product yield, ^b %						
				1	2	3	4	5	6	7
1	1 (125), Me ₂ SO ₄ (300), K ₂ CO ₃ (375)	acetone	5.5				47	<2	35	10
2	1 (125), Me ₂ SO ₄ (188), Cs ₂ CO ₃ (375)	MeCN	5	23	4		31	28	4	
3	1 (18), MeI (93), MeONa (44)	MeCN	8	12	24	<2	31	15	4	
4	1 (33), Me ₂ SO ₄ (40), CsF (167)	MeCN	9	26	23	6	14	4	7	<2
5	1 (27), Me ₂ SO ₄ (42), MeONa (113)	MeOH	4.5	42	25					
6	1 (22), Me ₂ SO ₄ (60), Me ₄ NOH (55)	dioxane	4		9	6	9	12	43	<2

^a At reflux temperature apart from the case of run 6 (50 °C). ^b ¹H NMR yields.

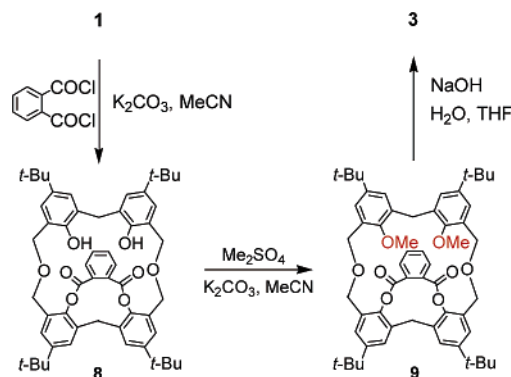
strong ligands could be obtained with its doubly bridged derivatives,⁶ and even the simple parent tetraphenol compound was found to bind quaternary ammonium ions.⁹ The apparently general ability of [3.1.3.1]homooxalixarene compounds to include suitable organic cations within their aromatic cavity, as compared with the relative difficulties often encountered with typical calixarenes,¹⁰ encouraged us to investigate other simple compounds featuring this macrocyclic system. In the frame of a systematic development of the chemistry of homooxalixarenes we now report on the formation, characterization, and complexation properties of the whole family of partially *O*-methylated *p*-*tert*-butyl[3.1.3.1]homooxalixarenes, compounds 2–6.



(7) (a) No, K.; Bok, J. H.; Suh, I. H.; Kang, S. O.; Ko, J.; Nam, K. C.; Kim, J. S. *J. Org. Chem.* **2004**, *69*, 6938. (b) No, K.; Lee, J. H.; Yang, S. H.; Noh, K. H.; Kim, S. K.; Seo, J.; Lee, S. S.; Kim, J. S. *J. Inclusion Phenom. Macrocyclic Chem.* **2003**, *47*, 167. (c) No, K.; Chung, H. J.; Yu, H. J.; Yang, S. H.; Noh, K. H.; Thuéry, P.; Vicens, J.; Kim, J. S. *J. Inclusion Phenom. Macrocyclic Chem.* **2003**, *46*, 97. (d) No, K.; Lee, Jeong H.; Yang, S. H.; Yu, Sang H.; Cho, M. H.; Kim, Moon J.; Kim, J. S. *J. Org. Chem.* **2002**, *67*, 3165. (e) No, K.; Park, Y. J. *Bull. Korean Chem. Soc.* **2002**, *23*, 1629. (f) No, K.; Lee, J. H.; Yang, S. H.; Noh, K. H.; Lee, S. W.; Kim, J. S. *Tetrahedron* **2003**, *59*, 2403. (g) No, K.; Park, Y. J.; Choi, E. J. *Bull. Korean Chem. Soc.* **1999**, *20*, 905. (h) No, K. H.; Kim, J. S.; Shon, O. J.; Yang, S. H.; Suh, I. H.; Kim, J. G.; Bartsch, R. A.; Kim, J. Y. *J. Org. Chem.* **2001**, *66*, 5976.

(8) No, K.; Lee, J. H. *Bull. Korean Chem. Soc.* **2000**, *21*, 1055.

SCHEME 1



Results and Discussion

Synthesis. Partial *O*-methylation of compound 1 has been carried out under several different conditions, and a rough estimate of the product distribution in selected cases is given by the ¹H NMR yields shown in Table 1. In a few cases only, evidence was obtained of the formation of small amounts of the dimethyl ether derivative 3; on the other hand, the dimethyl ether derivative 4 formed in almost all the tested conditions, in some instances in fairly good yields. High selectivity is seldom apparent in the data reported in Table 1. In general, column chromatography allowed to separate in pure form 1 and 2 but was unsuccessful for the other products. On the other hand, careful recrystallization of suitable reaction mixtures allowed 4 to be obtained in pure form and, after its removal, pure 5 and 6. An alternative synthesis was developed to obtain the elusive dimethyl ether derivative 3. According to Scheme 1, selective protection of 1 with phthaloyl dichloride followed by dimethylation of 8 and by alkaline hydrolysis of the resulting 9 afforded the desired compound 3. The phthaloyl bridging unit was chosen on the basis of modeling and of the reported regioselectivity in the reaction on *p*-*tert*-butylcalix[4]arene.^{11,12}

The composition of the reaction mixture in the direct methylation is affected by several factors. After monomethylation has occurred, three competing reactions can take place. In the analogous reaction on calixarenes and in other similar cases, the regioselectivity of the attack is usually interpreted

(9) Masci, B. *Tetrahedron* **1995**, *51*, 5459.

(10) Dalla Cort, A.; Mandolini, L. In *Calixarenes in Action*; Mandolini, L., Ungaro, R., Eds.; Imperial College Press: London, 2000.

(11) (a) Van Loon, J. D.; Kraft, D.; Ankoné, M. J. K.; Verboom, W.; Harkema, S.; Vogt, W.; Böhmer, V.; Reinhoudt, D. N. *J. Org. Chem.* **1990**, *55*, 5176. (b) Kraft, D.; Böhmer, V.; Vogt, W.; Ferguson, G.; Gallagher, J. F. *J. Chem. Soc., Perkin Trans. 1* **1994**, 1221.

(12) Disiloxane bridges have also been successfully employed for the selective protection of adjacent hydroxyl groups in calix[4]arenes and thiacalix[4]arenes; see: Narumi, F.; Morohashi, N.; Matsumura, N.; Iki, N.; Kameyama, H.; Miyano, S. *Tetrahedron Lett.* **2002**, *43*, 621.

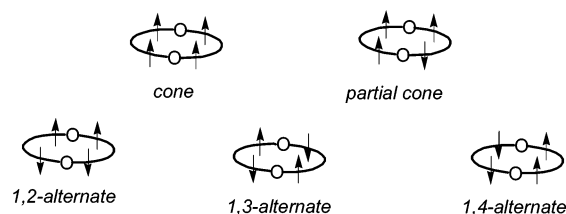


FIGURE 1. Schematic representation of the ideal conformations of [3.1.3.1]homooxalixarenes.

on the basis of the relative acid strength of the various ArOH functions as determined by the intramolecular hydrogen bonds.¹³ The picture is actually a complex one since the (mean) number of deprotonated phenol functions in a given solvent changes with the nature and with the concentration of the base, which is in most cases heterogeneous. Moreover, the correlation between the extent of deprotonation and the overall reactivity could in principle fail since the less stable phenoxide ion, despite its lower concentration, could turn out to be the most reactive one. The effects of association of the mono- or polyanion with one or more counterions are determinant both in the acid–base equilibria and in the nucleophilic substitution reactions. On the other hand, the relative abundance of the three dimethylated products is determined not only by their ease of formation but also by the rate of their further reaction to give the trimethyl ether **6**, which is the single compound formed from **3**, **4**, or **5**, indifferently.

Conformation in Solution. All compounds **1–7** are conformationally mobile in solution, and a rapid conformational interconversion takes place on the NMR time scale at room temperature. In this paper the conformations of [3.1.3.1]-homooxalixarenes will be indicated according to the previously reported general naming system for isosubstituted homooxalix[4]arenes,² Figure 1.¹⁴ In the presence of different substituents at the lower rim, as in the case of the present partially etherified compounds, the number of alternate conformations is the same as in isosubstituted compounds, but up to four different partial cone conformations occur, a complete picture being given in the Supporting Information.

The conformational analysis strongly relied on the chemical shift values in the ¹³C NMR spectra to distinguish between *syn*- and *anti*-arranged ArCH₂Ar units¹⁵ and on the chemical shift values in the ¹H NMR spectra to detect OCH₃ groups facing aromatic rings. ¹H NMR spectra at variable temperature were also recorded down to 177 K in CD₂Cl₂, at 300 MHz. The most important NMR spectral features and the results of the conformational analysis are reported in Table 2 along with the conformation determined in the solid state (see below). The intramolecular hydrogen bond is expected to play an important role in the conformation of **1–6**. Its strength influ-

ences the $\delta(\text{ArOH})$ values in the ¹H NMR spectra, which apparently decrease in the order **1** > **2** > **3–6** (column 2 in Table 2).

The spectra at low temperature, given in Figure 2 for compound **4** and in the Supporting Information for **2**, **3**, **5**, and **6**, indicated the presence of two different main conformations in the case of **2**, **4**, and **5**, and of only one main conformation in the case of **3**. In the case of **6** the large number of broad signals did not allow a safe analysis to be carried out. Not only do the singlets of the CH₂ protons in Figure 2 split into AX or AB systems on cooling, but also the OCH₃ singlet undergoes splitting into two singlets of quite different areas. The latter feature indicates that besides the prevailing cone conformation a small amount of an alternate conformation is present, whose small CH₂ signals cannot be detected. In general, the relative population of each conformation (column 5 in Table 2) was estimated both from the areas of the OCH₃ (or OH) peaks split at low temperatures and from the chemical shift of the split and nonsplit peaks below and above the coalescence temperature, respectively. The two methods gave results in substantially good agreement.

In no case were peaks at ca. 37–40 ppm indicating *anti*-arranged ArCH₂Ar units¹⁵ observed in the ¹³C NMR spectra, thus ruling out the prevalence of partial cone, 1,2-alternate, or 1,3-alternate conformations. In the case of **6** only one of the expected signals is apparent, at 30.9 ppm, the other probably being superimposed on the intense CH₃ signals in the same region. On the other hand, in the case of **3** one of the two expected signals appears in a somewhat atypical region, at about 33 ppm. The presence of a significant amount of one of the above conformations featuring *anti* arrangement for the ArCH₂-Ar units is nevertheless ruled out by the variable-temperature experiments, which clearly indicate the presence of only one main conformation, so in this case a significant distortion in one of the two *syn*-arranged ArCH₂Ar units is likely to take place.^{15b} Shielding of methyl protons in NMR spectra by facing aromatic rings is expected in noncone conformations and is used as a standard criterion, the reference value being at ca. 3.8 ppm for noncyclic compounds.⁴ We guess that the detected minor conformation is actually the 1,4-alternate, which is commonly observed in nonbridged [3.1.3.1]homooxalixarenes^{2,4,7e–g} and which is also found in most cases for **2–7** in the solid state. The latter assignment is in agreement with the observed unimportance of *anti*-arranged ArCH₂Ar units. In the case of compound **6** it should be noted that quite different δ values are observed for the three ArOCH₃ signals; in particular the signal at 3.76 ppm indicates the absence of facing aromatic rings. The naive conclusion that the cone conformation is present is obviously in contrast with the upfield shift experienced by the other two ArOCH₃ groups. Probably an intramolecular hydrogen bond with the proximal ArOH function turns the methoxy protons away from the aromatic ring.

The difference in the δ ArOCH₃ values in CDCl₃ and CD₂-Cl₂ solvents (Table 2) is smaller than 0.1 ppm for all ligands apart from **4** ($\Delta\delta = 0.25$). In the latter case the relative stability of the cone conformation is apparently higher in CDCl₃ than in CD₂Cl₂.

Crystal Structure. The crystal structures of compounds **2–7** were determined by single-crystal X-ray diffraction, whereas the structure of **1** in the cone conformation, as an acetonitrile, a pyridine, or a chloroform/tetrahydrofuran solvate, has been

(13) Seri, N.; Biali, S. *J. Org. Chem.* **2005**, *70*, 5278 and references therein.

(14) 1,2-Alternate and 1,4-alternate conformations are indicated by No et al.^{7a–f} as COC-1,2-alternate and C-1,2-alternate, respectively. The naming system proposed in ref 2 is intended to be useful for the conformations of isosubstituted homooxalix[4]arenes in general. Namely, analogous problems hold for [3.3.3.1]homooxalixarenes and for [3.1.1.1]homooxalixarenes. In the latter case, 1,2-alternate and 1,4-alternate conformations according to ref 2 are otherwise named 1,2-alternate A and 1,2-alternate B; see: Félix, S.; Ascenso, J. R.; Lamartine, R.; Pereira, J. L. C. *Tetrahedron* **1999**, *55*, 8539.

(15) (a) Jaime, C.; De Mendoza, J.; Prados, P.; Nieto, P. M. *J. Org. Chem.* **1991**, *56*, 3372. (b) Magrans, J. O.; De Mendoza, J.; Pons, M.; Prados, P. *J. Org. Chem.* **1997**, *62*, 4518.

TABLE 2. Relevant NMR Spectral Data and Results of the Conformational Analysis for Compounds 1–7

ligand	$\delta(\text{ArOH})^a$ in CDCl_3	$\delta(\text{ArOCH}_3)^a$ in CDCl_3 (in CD_2Cl_2)	$\delta(\text{ArCH}_2\text{Ar})^b$ in CDCl_3	conformation in CD_2Cl_2	conformation in the solid state
1	8.97		31.3	cone ^c	cone ^d
2	8.28 (2H), 8.00(1H)	3.83 (3.85)	29.7, 31.2	cone, 93%; 1,4-alternate, 7%	1,4-alternate
3	7.60	3.32 (3.24)	30.6, 33.2	1,4-alternate	partial cone ^e
4	7.49	3.40 (3.65)	30.1	cone, 87%; 1,4-alternate, 13%	1,4-alternate
5	7.39	3.45 (3.54)	30.6	cone, 62%; 1,4-alternate, 38%	1,4-alternate
6	7.48	3.01, 3.37, 3.76 (2.97, 3.36, 3.71)	30.9 ^f	g	1,4-alternate
7		3.16 (3.10) ^h	31.2 ^h	1,4-alternate ^h	1,4-alternate

^a ¹H NMR spectra. ^b ¹³C NMR spectra. ^c From ref 16. ^d From ref 17. ^e $3 \cdot \text{CHCl}_3 \cdot \text{H}_2\text{O} \cdot 0.5\text{MeOH}$ solvate. ^f The second expected signal is not apparent. ^g The main conformation is probably 1,4-alternate. ^h Data from ref 4.

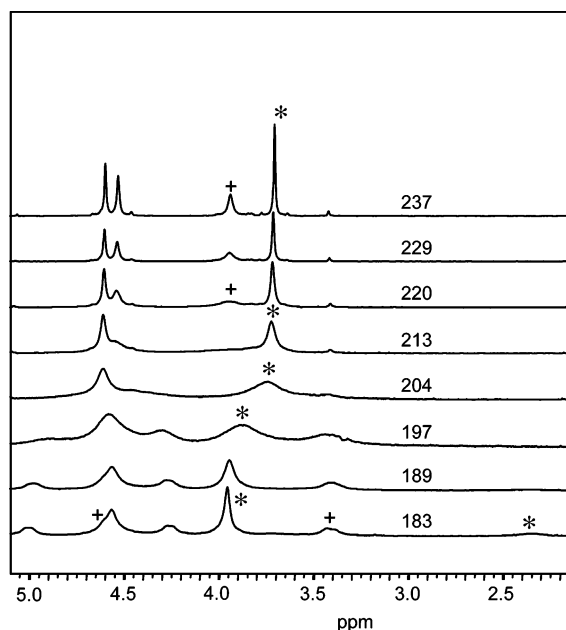


FIGURE 2. ¹H NMR spectra (central region) of compound 4 at low temperatures, in CD_2Cl_2 . Symbols mark the proposed splitting pattern for OCH_3 protons (*) and ArCH_2Ar protons (+).

reported previously.¹⁷ The present structures indicate the 1,4-alternate conformation of compounds 2 and 4–7, and the partial cone conformation of 3 in its solvate $3 \cdot \text{CHCl}_3 \cdot \text{H}_2\text{O} \cdot 0.5\text{MeOH}$ (Figures 3–8 for compounds 2–7, respectively). The macrocycles in 2, 4, 6, and 7 admit a crystallographic inversion center with, as a consequence, one methoxy carbon atom being disordered over two symmetry-related positions in the mono- and trimethoxy derivatives 2 and 6. The macrocycles in $3 \cdot \text{CHCl}_3 \cdot \text{H}_2\text{O} \cdot 0.5\text{MeOH}$ and 5 do not possess any crystallographic symmetry. Intramolecular hydrogen bonds stabilize the conformation (except in 7 and possibly in 6), the acceptor atoms being phenolic, methoxy, or ether oxygen atoms. The two C–O–C–C torsion angles defined by each ether bridge are *gauche/anti* for all the macrocycles in the 1,4-alternate conformation, whereas they are *anti/anti* in the partial cone compound 3. In the latter case, the bridges adopt a quasi-planar “w” shape.

Complexation of Quaternary Ammonium Ions. Complexation of quaternary ammonium ions in apolar solvents is a suitable test of the shape and size of the potential cavity of a

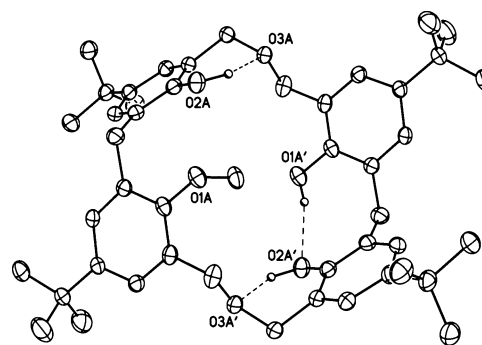


FIGURE 3. View of one of the two independent molecules in compound 2. Only one of the positions for the disordered groups is represented. Hydrogen bonds are represented as dashed lines. Symmetry code: prime = $2 - x, 1 - y, -z$.

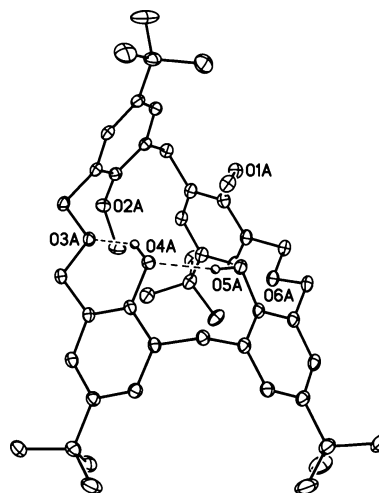


FIGURE 4. View of one of the two independent molecules in compound $3 \cdot \text{CHCl}_3 \cdot \text{H}_2\text{O} \cdot 0.5\text{MeOH}$. Only one of the positions for the disordered groups is represented. Hydrogen bonds are represented as dashed lines.

neutral cyclophane. In the absence of hydrophobic interactions and hydrogen bond or ion pairing with the ligand, complexation is mainly based on cation– π interaction,¹⁸ and it actually tests the ability of the ligand to expose several aromatic faces to the included cationic guest. Several calixarene and calixarene-like cyclophanes have been reported to bind quaternary ammonium ions,^{10,19} a distinct role being played in the field by homooxalixarenes.^{2,4,6,9,10} In particular, in a previous investigation in

(16) Gutsche, C. D.; Bauer, L. J. *J. Am. Chem. Soc.* **1985**, *107*, 6052.
(17) (a) Thuéry, P.; Nierlich, M.; Vicens, J.; Masci, B.; Takemura, H. *Eur. J. Inorg. Chem.* **2001**, 637. (b) Thuéry, P.; Nierlich, M.; Vicens, J.; Masci, B. *Acta Crystallogr., Sect. C* **2001**, *57*, 70.

(18) (a) Ma, J. C.; Dougherty, D. A. *Chem. Rev.* **1997**, *97*, 1303. (b) Dougherty, D. A.; Zacharias, N. *Trends Pharmacol. Sci.* **2002**, *23*, 281. (c) Cashin, A. L.; Petersson, E. J.; Lester, H. A.; Dougherty, D. A. *J. Am. Chem. Soc.* **2005**, *127*, 350.

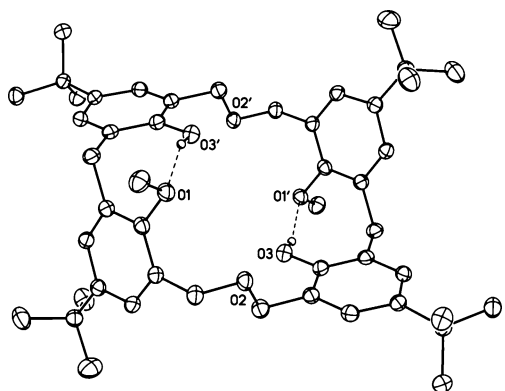


FIGURE 5. View of molecule **4**. Hydrogen bonds are represented as dashed lines. Symmetry code: prime = $1 - x, 2 - y, 2 - z$.

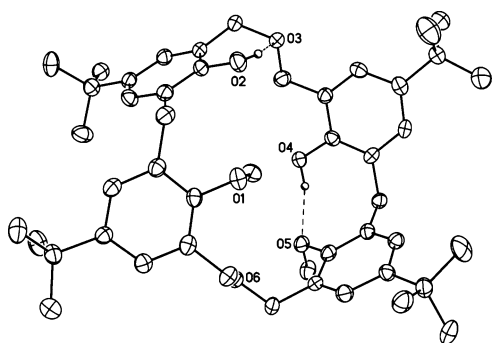


FIGURE 6. View of molecule **5**. Hydrogen bonds are represented as dashed lines.

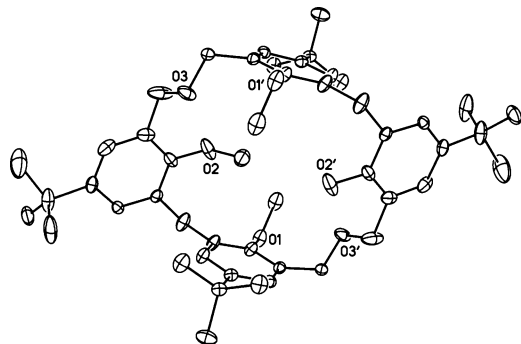


FIGURE 7. View of molecule **6**. Only one of the positions for the disordered groups is represented. Symmetry code: prime = $1 - x, 1 - y, 2 - z$.

halogenated solvents on the series of tetramethyl ether derivatives of *p*-*tert*-butylhomooxalix[4]arenes,⁴ **7** proved to be the most effective ligand for tetramethylammonium picrate (TMAP). We now report on the complexation of four different salts, namely, TMAP, tetraethylammonium picrate (TEAP), *N*-methylpyridinium picrate (NMPP), and acetylcholine picrate (ACP), by the whole family of ligands **1–7** in CDCl₃ at 298 K. The

(19) (a) Arduini, A.; Demuru, D.; Pochini, A. *Chem. Commun.* **2005**, 645. (b) Arduini, A.; Brindani, E.; Giorgi, G.; Pochini, A.; Secchi, A. *J. Org. Chem.* **2002**, *67*, 6188. (c) Arduini, A.; Giorgi, G.; Pochini, A.; Secchi, A.; Ugozzoli, F. *J. Org. Chem.* **2001**, *66*, 8302. (d) Arduini, A.; Pochini, A.; Secchi, A. *Eur. J. Org. Chem.* **2000**, 2325. (e) Böhmer, V.; Dalla Cort, A.; Mandolini, L. *J. Org. Chem.* **2001**, *66*, 1900. (f) Arnecke, R.; Böhmer, V.; Cacciapaglia, R.; Dalla Cort, A.; Mandolini, L. *Tetrahedron* **1997**, *53*, 4901. (g) Tran, A. H.; Miller, D. O.; Georghiou, P. E. *J. Org. Chem.* **2005**, *70*, 1115.

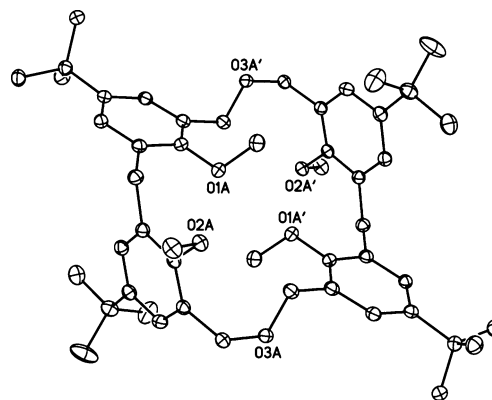


FIGURE 8. View of one of the two independent molecules in **7**. Symmetry code: prime = $0.5 - x, 0.5 - y, 2 - z$.

TABLE 3. Association Constants of Ligands **1–7** and Limiting Upfield Shifts in the ¹H NMR Spectra of the Included Cation^a

1	15 	15 	30 ^{1.6} 	10
2	110 	40 	120 ^{1.7} 	60
3	130 	11 	90 ^{1.4} 	55
4	740 	15 	130 ^{1.5} 	190
5	410 	7 	80 ^{1.2} 	110
6	490 	4 	70 ^{0.9} 	140
7	220 	3 	25 ^{1.2} 	75

^a Picrate salts, in CDCl₃, at 298 K. Association constants (L mol⁻¹) are given in Roman type and $\Delta\delta_{\infty}$ (ppm) values in italic type.

technique used has been reported previously.^{4,9} The ¹H NMR spectra of the salt (0.13 mmol L⁻¹ for TMAP, 0.40 mmol L⁻¹ for ACP, and 1.00 mmol L⁻¹ for NMPP and TEAP) were recorded in the absence and in the presence of varying concentrations of the ligand. The association constants for 1:1 complexation and the $\Delta\delta_{\infty}$ values, namely, the limiting upfield shifts for the several protons of the included cation as obtained by the multiparameter least-squares treatment, are reported in Table 3, while the effects of the structure of the host and of the guest on the association strength are graphically reported in Figure 9. The abscissa in Figure 9 corresponds to the increase in the number of OCH₃ groups and to the decrease in the number of OH groups, but the sequence **3, 4, and 5** for the three dimethyl ether derivatives is actually an arbitrary one.

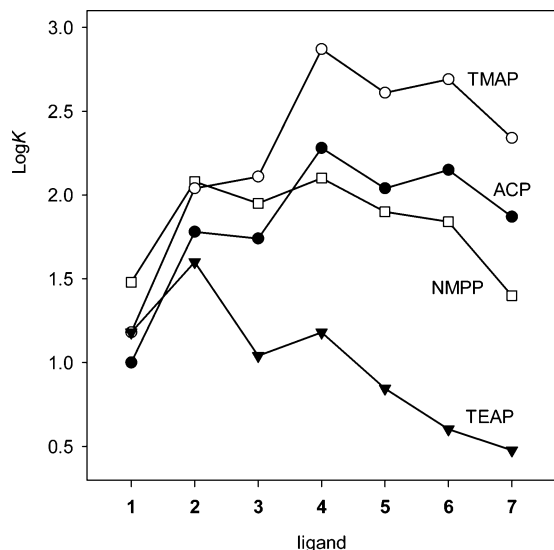


FIGURE 9. Association strength of ligands 1–7 with quaternary ammonium ions, in CDCl_3 at 298 K.

Several of the observed association constants are fairly good when allowance is made for the simplicity of the ligands, namely, for the absence of peculiar substituents and of bridging units to rigidify the structure. The limiting shielding effects of the aromatic clouds on the protons of the included cation are in most cases in the range 1–2 ppm, while small effects, $\Delta\delta_\infty$ values in the range 0.04–0.12 ppm, were observed for picrate counterion. The rather low $\Delta\delta_\infty$ values for the tail of the cation in ACP clearly indicate that it is substantially out of the aromatic cavity in the complex, nevertheless with a significant trend from 1 to 7. On the other hand, the somewhat low $\Delta\delta_\infty$ values observed in some cases with TEAP indicate an only partial inclusion of the large cation, with relatively low mean weighed effects. The highest observed association value (ligand 4 with TMAP) corresponds to a high $\Delta\delta_\infty$ value, but with the present unpreorganized ligands a precise correlation between observed binding and shielding effects cannot be expected.

The strongest complexes are formed with the small TMA ion and the weakest ones with the large TEA ion. Moreover, in the case of ligands 1 and 2, for instance, the strongest complexes are formed with NMP ion, while TMA and AC are best complexed by ligand 4. On changing the ligand structure, almost regular profiles and trends are observed in Figure 9, but important selectivity features can be better appreciated on inspection of Figures 10 and 11. In Figure 10 $\log K$ values relative to those observed with TMAP are reported as a function of the cation structure, while in Figure 11 the values relative to those observed with TMAP are normalized by the values relative to those observed with TMAP for ligand 1 and plotted as a function of the ligand structure. The crossing of the profiles observed in Figure 9 appears to be less important in Figure 10 and is completely absent in Figure 11. Figures 10 and 11 clearly indicate that the selectivity in complexation increases in the order $1 < 2 < 3 < 4-7$.

To rationalize the observed trends, the following points should be taken into account. The macrocyclic system is the same in compounds 1–7, so the cavity featuring the aromatic walls can in principle be arranged in the same fashion to encircle a given guest cation. If this is the case, different reorganization energies but the same cation– π interaction and the same limiting shielding effects on a given included salt are expected for the

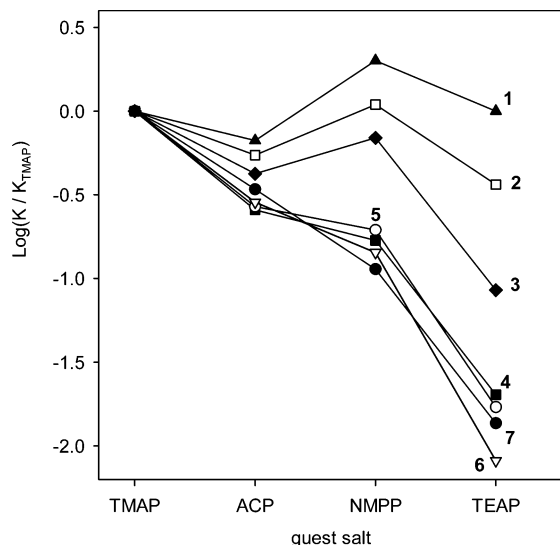


FIGURE 10. Selectivity in the binding of quaternary ammonium salts by ligands 1–7: binding of the various guest salts relative to TMAP.

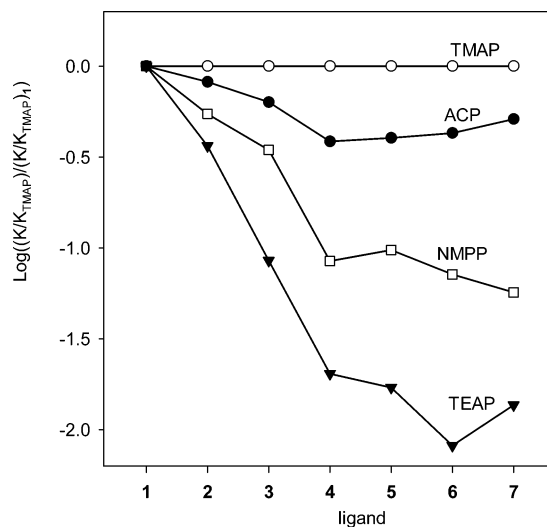


FIGURE 11. Selectivity in the binding of quaternary ammonium salts by ligands 1–7: relative response of the various guest salts to changes in the structure of the ligand.

various ligands. It is apparent from the values in the columns of Table 3 that significant differences in $\Delta\delta_\infty$ occur in several instances, so the cavity must be somewhat differently arranged in the various complexes with the same salt, as the result of a balance between cation– π interaction and strain energy. However, we can safely assume that differences in geometry are much smaller in the complexes than in the free ligands; in particular a cone geometry is reasonably required in all the complexes. On the other hand, in a severely distorted or flattened cone the four aromatics cannot strongly interact with the included cation. In the absence of covalent bridges and of huge or peculiarly conjugated substituents at the lower rim, the intramolecular hydrogen bonding is the fundamental structural feature to differentiate the ligands, and it should largely account for the varying reorganization energy. Ligand 1 is in the cone conformation in solution, but the crystal structure suggests that it is actually a flattened and distorted cone that requires heavy reorganization of the hydrogen bonds to feature a deeper cavity and to better interact with the small TMA ion. The $\Delta\delta_\infty$ value

indicates that the four aromatic clouds are not interacting as strongly as in the case of complexes **2**–**7**. The larger TEA and NMP ions that can interact on a large surface are not handicapped in this case. In the case of ligand **7**, at the other extreme in the series, no hydrogen bond organizes the cavity and the free ligand is arranged in the 1,4-alternate conformation, with no detectable presence of the cone conformation. The conformational handicap to reach the cone conformation must then be significant, but the cone can be easily adapted to make the four aromatic clouds effectively encircle the small TMA ion, while the large TEA and NMP ions cannot enter the cavity, which is narrower than the cavity of **1**, in depth. On increasing the number of methoxy groups and decreasing the number of hydrogen bonds, a continuous change in the geometry of both the free and the complexed ligand can be expected in the series **1**–**7**. The relative stability of the cone conformation in solution is found to actually decrease in the order $1 > 2 > 5 > 4 > 3 \approx 7$, the picture for **6** probably being close to that observed for **3** and **7**. On the other hand, the importance of the hydrogen bonding that can distort or flatten the cone conformation is expected to roughly follow the inverted order. The observed order of K values is the result of a balance of the above factors, which can be finely tuned in the present series.

Conclusions

Conditions have been found to obtain the whole family of the products of partial *O*-methylation of *p*-*tert*-butyl[3.1.3.1]-homooxacalixarene. All the compounds are in the 1,4-alternate conformation in the solid state, apart from the diether **3** for which a partial cone conformation has been determined in a solvate. In halogenated solvents the relative stability of the cone conformation with respect to the 1,4-alternate conformation decreases on increasing the number of ether functions. A systematic investigation in CDCl_3 of the binding with four quaternary ammonium salts featuring the same counterion has been carried out on the complete series of ligands **1**–**7** in which the structure is finely tuned from the tetraphenol to the tetraether. The overall observed association constants are the result of several interactions that are difficult to estimate; in particular, changes in solvation, in cation–anion attraction, and in conformational energy are superimposed on those in cation– π attraction. The systematic investigation of the present family of strictly related compounds allows several of these factors to be largely neglected in the comparison. If roughly similar changes in solvation and in cation–anion attraction are assumed in the complexation of a given salt by **1**–**7**, the results of the conformational analysis on the free ligands allow the contribution of the reorganization energy and of the cation– π attraction to be somewhat separated. On the other hand, the response of the various ligands to changes in the structure of the cation guest indicates that the cone conformations are somewhat differently arranged or differently rigid, the observed trend indicating that the bulkier the guest, the heavier the handicap for the ligands featuring few ArOH functions and few intramolecular hydrogen bonds. We can conclude that the shape of the ligands in the complexes is largely determined by the intramolecular hydrogen bonds that flatten (and possibly distort) the cone, thus affecting the ligand selectivity according to the schematic picture in Figure 12.

Experimental Section

Complexation Experiments. Reference is made to previous papers^{4,9} for the titration technique and data treatment in complex-

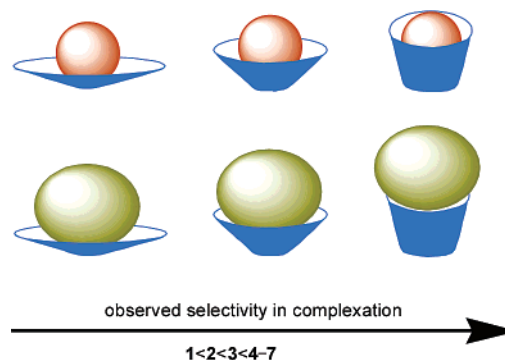


FIGURE 12. Schematic representation of the increase in the ligand selectivity and in the depth of the cone conformation along the series **1**–**7**.

ation experiments. For K larger than 10 L mol^{-1} reproducibility of the data is within 10% for both the K and $\Delta\delta_\infty$ parameters, while the multiple fit procedure afforded the parameters with a standard deviation lower than 2%. In the case of the weakest associations the uncertainty on the parameters can be estimated to be on the order of 25%.

Quantitative Product Analysis. Quantitative analysis of the mixtures of methyl ether derivatives was mainly carried out through ^1H NMR spectra taken in CDCl_3 . ArOH and OCH_3 peaks were integrated in spectra of samples prepared from an aliquot of the final reaction mixture in the presence of *p*-*tert*-butylcalix[4]arene as a standard. HPLC analyses were unfortunately of less general applicability, due to some peak superimposition in all the tested conditions. HPLC data (when available) were in substantial agreement with the results of the ^1H NMR analysis. Preparative yields of pure isolated products and the composition of recovered simplified mixtures after column chromatography and/or recrystallization also substantially confirmed the ^1H NMR results on the crude.

General Procedure for the Methylation of 1. A mixture of **1**, the base, and the methylating agent was refluxed (heated at 50°C in run 6 in Table 1) and stirred under a nitrogen atmosphere. In run 4 the mixture of CsF, **1**, and MeCN was refluxed and stirred for 1 h before addition of Me_2SO_4 . The solvent was then evaporated, water was added, and the mixture was neutralized (HCl) and extracted with CHCl_3 . After washing with water and drying, an aliquot of the CHCl_3 solution was taken in several cases for the quantitative analysis and the remaining part evaporated. The residue was subjected to column chromatography (SiO_2 , eluent toluene/ CHCl_3 , 2:1). Compounds **1** and **2** were eluted in order in pure form, and then the unresolved mixture of the remaining methyl ether derivatives was eluted. Attempted separation of the latter compounds with different eluents and/or different batches of silica or alumina was unsatisfactory; nevertheless, pure samples of compounds **4**–**6** could be obtained through careful recrystallization of suitable mixtures. In some cases, column chromatography was skipped and recrystallization was carried out directly on the residue. Representative procedures to obtain pure samples of **2** and of **4**–**6** are given below and in the Supporting Information, respectively.

7,13,21,27-Tetra-*tert*-butyl-29,30,31-trihydroxy-32-methoxy-2,3,16,17-tetrahydro-3,17-dioxacalix[4]arene (2). A mixture of **1** (287 mg, 0.405 mmol), MeONa (91.5 mg, 1.69 mmol), and Me_2SO_4 (79.8 mg, 0.633 mmol) was reacted in MeOH (15 mL) for 4.5 h (run 5 in Table 1). After the usual workup column chromatography of the residue yielded unreacted **1** (110 mg, 38%) and **2** (82 mg, 28%), which was recrystallized from hexane for analytical purposes: mp 201 – 203°C ; MS (ES^-) m/z 721.6 [$\text{M} - \text{H}$]; ^1H NMR δ 1.22 (s, 9H), 1.23 (s, 9H), 1.26 (s, 9H), 1.30 (s, 9H), 3.83 (s, 3H), 3.88 (s, 2H), 4.02 (s, 2H), 4.48 (s, 2H), 4.59 (s, 2H), 4.65 (s, 2H), 4.72 (s, 2H), 6.94–6.98 (overlapped, 3H), 7.10 (d, $J = 2.6 \text{ Hz}$, 1H), 7.21 (d, $J = 2.4 \text{ Hz}$, 1H), 7.27 (d, $J = 2.6 \text{ Hz}$, 1H),

7.31 (d, $J = 2.6$ Hz, 1H), 7.33 (d, $J = 2.6$ Hz, 1H), 8.00 (s, 1H), 8.27 (s, 2H); ^{13}C NMR δ 29.7, 31.2, 31.3, 31.4, 31.5, 31.6, 33.9, 33.9, 34.2, 61.6, 70.2, 70.4, 71.8, 72.4, 122.4, 122.8, 123.4, 124.1, 124.4, 125.1, 125.8, 127.3, 127.4, 127.6, 127.9, 128.1, 128.6, 134.0, 141.7, 142.7, 143.0, 146.7, 150.0, 150.6, 152.2, 154.1. Anal. Calcd for $\text{C}_{47}\text{H}_{62}\text{O}_6$: C, 78.08; H, 8.64. Found: C, 77.97; H, 9.01.

Data for 7,13,21,27-tetra-*tert*-butyl-29,31-dihydroxy-30,32-dimethoxy-2,3,16,17-tetrahydro-3,17-dioxacalix[4]arene (4): isolated in 51% yield; mp 236–237 °C; MS (ES^-) m/z 735.7 [$\text{M} - \text{H}$]; ^1H NMR δ 1.28 (s, 18H), 1.28 (s, 18H), 3.40 (s, 6H), 3.87 (s, 4H), 4.45 (s, 4H), 4.68 (s, 4H), 7.01 (d, $J = 2.4$ Hz, 2H), 7.23 (d, $J = 2.3$ Hz, 2H), 7.25 (d, $J = 2.3$ Hz, 2H), 7.28 (d, $J = 2.4$ Hz, 2H), 7.39 (s, 2H); ^{13}C NMR δ 30.1, 31.4, 31.6, 33.9, 34.3, 61.7, 67.2, 70.7, 123.1, 124.7, 125.5, 127.4, 127.4, 127.7, 129.7, 133.5, 142.1, 147.1, 150.8, 153.0. Anal. Calcd for $\text{C}_{48}\text{H}_{64}\text{O}_6$: C, 78.22; H, 8.75. Found: C, 77.82; H, 8.99.

Data for 7,13,21,27-tetra-*tert*-butyl-29,30-dihydroxy-31,32-dimethoxy-2,3,16,17-tetrahydro-3,17-dioxacalix[4]arene (5): isolated in 14% yield; mp 227–228 °C; MS (ES^-) m/z 735.7 [$\text{M} - \text{H}$]; ^1H NMR δ 1.25 (s, 18H), 1.27 (s, 18H), 3.45 (s, 6H), 3.84 (s, 4H), 4.49 (s, 4H), 4.64 (s, 4H), 7.08 (d, $J = 2.3$ Hz, 2H), 7.18–7.21 (overlapped, 4H), 7.24 (d, $J = 2.3$ Hz, 2H), 7.49 (s, 2H); ^{13}C NMR δ 30.6, 31.3, 31.6, 34.0, 34.2, 62.2, 67.3, 70.3, 123.2, 123.9, 126.8, 127.2, 127.4, 127.8, 129.4, 133.6, 142.3, 146.9, 150.4, 153.7. Anal. (agrees with data for $5 \cdot 1.5\text{H}_2\text{O}$) Calcd for $\text{C}_{48}\text{H}_{67}\text{O}_{7.5}$: C, 75.46; H, 8.84. Found: C, 75.66; H, 8.83.

Data for 7,13,21,27-tetra-*tert*-butyl-29-hydroxy-30,31,32-trimethoxy-2,3,16,17-tetrahydro-3,17-dioxacalix[4]arene (6): isolated in 22% yield; mp 168–169 °C; MS (ES^-) m/z 749.7 [$\text{M} - \text{H}$]; ^1H NMR δ 1.18 (s, 9H), 1.23 (s, 9H), 1.28 (s, 9H), 1.29 (s, 9H), 3.02 (s, 3H), 3.37 (s, 3H), 3.76 (s, 3H), 3.80 (s, 2H), 3.93 (s, 2H), 4.47 (s, 2H), 4.52 (s, 4H), 4.57 (s, 2H), 7.05–7.08 (overlapped, 2H), 7.17–7.20 (overlapped, 3H), 7.21 (d, $J = 2.6$ Hz, 1H), 7.24 (d, $J = 2.6$ Hz, 1H), 7.26–7.28 (overlapped, 1H), 7.48 (s, 1H); ^{13}C NMR δ 30.9, 31.3, 31.3, 31.4, 31.5, 33.9, 34.2, 34.2, 61.6, 62.2, 62.2, 66.4, 66.9, 68.6, 70.0, 123.8, 124.8, 125.6, 126.7, 126.7, 127.1, 127.1, 127.7, 128.3, 128.4, 129.9, 129.9, 130.1, 133.0, 134.0, 134.1, 142.0, 145.9, 146.1, 147.0, 150.7, 152.3, 155.1, 155.4. Anal. Calcd for $\text{C}_{49}\text{H}_{66}\text{O}_6$: C, 78.36; H, 8.86. Found: C, 78.21; H, 9.20.

7,13,21,27-Tetra-*tert*-butyl-29,32-dihydroxy-30,31-phthaloyl-dioxy-2,3,16,17-tetrahydro-3,17-dioxacalix[4]arene (8): A mixture of **1** (400 mg, 0.56 mmol) and K_2CO_3 (280 mg, 2.03 mmol) in CH_3CN (25 mL) was refluxed for 30 min, and then a solution of *o*-phthaloyl dichloride (133 mg, 0.65 mmol) in CH_3CN (10 mL) was added dropwise in 5 h. After 2 days of further refluxing and stirring, diluted HCl and CHCl_3 (80 mL) were added, the organic layer was washed with water, dried, and evaporated, then 2 mL of CHCl_3 was added to the residue, and the mixture was stirred at room temperature. The undissolved material, consisting in the doubly bridged compound, was removed, while the filtrate was subjected to column chromatography (SiO_2 , eluent CHCl_3) to give **8** (96 mg, 20% yield): mp 281–283 °C; MS (ES^-) m/z 837.7 [$\text{M} - \text{H}$]; the ^1H NMR spectra at room temperature showed several broad peaks; ^1H NMR (in $\text{CDCl}_2\text{CDCl}_2$ at 350 K) δ 1.26 (s, 18H), 1.36 (s, 18H), 3.40 (d, $J = 13.5$ Hz, 1H), 3.42 (d, $J = 13.5$ Hz, 1H), 4.10 (d, $J = 13.5$ Hz, 1H), 4.14 (d, 1H, $J = 13.5$ Hz, 1H), 4.22 (d, $J = 12.6$ Hz, 2H), 4.34 (d, $J = 11.7$ Hz, 2H), 4.58 (d, $J = 11.7$ Hz, 2H), 4.78 (d, $J = 12.6$ Hz, 2H), 6.89 (d, $J = 2.3$ Hz, 2H), 6.92 (br s, 4H), 7.14 (d, $J = 2.3$ Hz, 2H), 7.32 (d, $J = 2.2$ Hz, 2H), 7.19–7.24 (m, 4H), 7.45 (d, $J = 2.2$ Hz, 2H), 7.58 (s, 2H); ^{13}C NMR (in $\text{CDCl}_2\text{CDCl}_2$ at 350 K) δ 31.2, 31.4, 31.7, 32.2, 33.9, 34.5, 68.4, 69.6, 122.8, 124.4, 125.9, 126.6, 127.6, 128.1, 128.4, 130.0, 131.1, 132.6, 142.9, 143.7, 149.7, 150.0, 163.9. Anal. Calcd for $\text{C}_{54}\text{H}_{62}\text{O}_8$: C, 77.30; H, 7.45. Found: C, 77.02; H, 7.80.

7,13,21,27-Tetra-*tert*-butyl-29,32-dimethoxy-30,31-phthaloyl-dioxy-2,3,16,17-tetrahydro-3,17-dioxacalix[4]arene (9): A mixture of **8** (100 mg, 0.119 mmol), K_2CO_3 (66 mg, 0.48 mmol), and Me_2SO_4 (30 mg, 0.24 mmol) in boiling MeCN (5 mL) was stirred and refluxed for 24 h. After the usual workup the residue was recrystallized from $\text{CHCl}_3/\text{MeOH}$ to give **9** (72 mg, 70% yield): mp 288–290 °C; MS (ES^+) m/z 889.5 [$\text{M} + \text{Na}$], 905.5 [$\text{M} + \text{K}$]; ^1H NMR δ 1.20 (s, 18H), 1.33 (s, 18H), 3.01 (s, 6H), 3.49 (d, $J = 13.8$ Hz, 1H), 3.64 (d, $J = 14.4$ Hz, 1H), 3.92 (d, $J = 13.8$ Hz, 1H), 4.02 (d, $J = 14.4$ Hz, 1H), 4.32 (d, $J = 11.0$ Hz, 2H), 4.35 (d, $J = 12.5$ Hz, 2H), 4.54 (d, $J = 12.5$ Hz, 2H), 4.63 (d, $J = 11.0$ Hz, 2H), 7.16 (apparent s, 4H), 7.35 (d, $J = 2.4$ Hz, 2H), 7.38 (d, $J = 2.4$ Hz, 2H), 7.59–7.65 (m, 2H), 7.69–7.75 (m, 2H); ^{13}C NMR δ 31.4, 31.4, 32.1, 33.3, 34.1, 34.5, 61.5, 66.5, 67.2, 125.3, 126.1, 127.3, 128.1, 129.5, 129.7, 130.4, 131.0, 131.5, 131.7, 134.1, 143.7, 145.8, 149.3, 155.1, 165.3. Anal. (agrees with data for $9 \cdot 0.5\text{H}_2\text{O}$) Calcd for $\text{C}_{56}\text{H}_{67}\text{O}_{8.5}$: C, 76.77; H, 7.71. Found: C, 76.89; H, 8.09.

7,13,21,27-Tetra-*tert*-butyl-29,32-dihydroxy-30,31-dimethoxy-2,3,16,17-tetrahydro-3,17-dioxacalix[4]arene (3): A mixture of **9** (67 mg, 0.077 mmol) and of 0.85 M NaOH in MeOH (3 mL) in THF (15 mL) was refluxed for 6 h. The residue obtained after the usual workup was recrystallized from $\text{CHCl}_3/\text{MeOH}$ to give **3** (30 mg, 53% yield): mp 118–120 °C; MS (ES^-) m/z 735.7 [$\text{M} - \text{H}$]; ^1H NMR δ 1.24 (s, 18H), 1.28 (s, 18H), 3.32 (s, 6H), 3.79 (s, 2H), 4.02 (s, 2H), 4.55 (s, 4H), 4.56 (s, 4H), 6.97 (d, $J = 2.3$ Hz, 2H), 7.19 (overlapped, 4H), 7.31 (d, $J = 2.4$ Hz, 2H), 7.61 (s, 2H); ^{13}C NMR δ 30.6, 31.4, 31.5, 33.2, 33.9, 34.2, 61.9, 69.1, 70.4, 123.1, 124.3, 126.8, 127.3, 127.7, 129.1, 129.6, 134.3, 142.6, 146.3, 150.1, 155.6. Anal. Calcd for $\text{C}_{48}\text{H}_{64}\text{O}_6$: C, 78.22; H, 8.75. Found: C, 77.91; H, 8.82.

Crystallographic Data Collection and Structure Determinations. The data were collected at 100(2) K on a Nonius Kappa-CCD area detector diffractometer²⁰ using graphite-monochromated Mo $\text{K}\alpha$ radiation ($\lambda = 0.71073$ Å). The data were processed with DENZO and SCALEPACK (HKL2000 package).²¹ The structures were solved by direct methods with SHELXS-97 and subsequent Fourier-difference synthesis and refined by full-matrix least squares on F^2 with SHELXL-97.²² No absorption correction was necessary. All non-hydrogen atoms were refined with anisotropic displacement parameters. Carbon-bound hydrogen atoms were introduced at calculated positions and were treated as riding atoms (as well as the oxygen-bound hydrogen atoms, when found) with a displacement parameter equal to 1.2 (OH, CH, CH_2) or 1.5 (CH_3) times that of the parent atom.

Acknowledgment. A financial contribution from MIUR COFIN 2003 is acknowledged.

Supporting Information Available: General methods for the experimental procedures, synthesis of compounds **4–6**, ^1H and ^{13}C NMR spectra of compounds **1–9**, low-temperature ^1H NMR spectra of compounds **2**, **3**, **5**, and **6**, complete list of the conformations of compounds **1–7**, crystal structure determination details and structural parameters, and tables of crystal and refinement data, atomic positions and displacement parameters, anisotropic displacement parameters, and bond lengths and bond angles in CIF format. This material is available free of charge via the Internet at <http://pubs.acs.org>.

JO051922T

(20) Kappa-CCD Software, Nonius B.V., Delft, The Netherlands, 1998.

(21) Otwinowski, Z.; Minor, W. *Methods Enzymol.* **1997**, 276, 307.

(22) Sheldrick, G. M. SHELXS-97 and SHELXL-97, University of Göttingen, Germany, 1997.